

Anomalous localization and duality in non-Hermitian quasiperiodic models

Wenzhi Wang,¹ Tianyu Li,^{2,3,*} and Wei Yi^{1,4,5,6,†}

¹Laboratory of Quantum Information, University of Science and Technology of China, Hefei 230026, China

²Key Laboratory of Atomic and Subatomic Structure and Quantum Control (Ministry of Education), Guangdong Basic Research Center of Excellence for Structure and Fundamental Interactions of Matter, School of Physics, South China Normal University, Guangzhou 510006, China

³Guangdong Provincial Key Laboratory of Quantum Engineering and Quantum Materials, Guangdong-Hong Kong Joint Laboratory of Quantum Matter, Frontier Research Institute for Physics, South China Normal University, Guangzhou 510006, China

⁴Anhui Province Key Laboratory of Quantum Network, University of Science and Technology of China, Hefei 230026, China

⁵CAS Center For Excellence in Quantum Information and Quantum Physics, Hefei 230026, China

⁶Hefei National Laboratory, University of Science and Technology of China, Hefei 230088, China

Boundary conditions can have dramatic impact in non-Hermitian systems, as exemplified by the non-Hermitian skin effect. Focusing on one-dimensional non-Hermitian quasiperiodic lattices, we show that the interplay of quasiperiodicity and the non-Hermitian skin effect leads to counterintuitive localization properties. On the one hand, for Anderson localized states under the periodic boundary condition, we find that their localization features can be boundary-sensitive, which originates from the incompatibility of the periodic boundary condition with quasiperiodicity. On the other hand, for non-localized states, the well-known extended-localized duality relation can break down, as their counterparts in the dual model can also be nonlocal. We discuss how these remarkable phenomena can be engineered and analyzed from the perspective of Lyapunov exponents. Our findings shed new light on localization in non-Hermitian quasiperiodic systems.

Introduction.— Anderson localization is a fundamental paradigm in physics, where wave propagations are localized by disorder [1–5]. In quasiperiodic lattice models, Anderson localization also arises, often accompanied by the localization-delocalization transition [6–12]. Take the Aubry-André-Harper model for instance [13–15]. The critical point for the transition is identified through self-duality, where the model Fourier transforms into itself. Away from the self-dual critical point, an extended-localized duality relation persists, under which an extended state is mapped to a localized one in the dual model, and vice versa [13, 16, 17]. Such a duality relation has been considered as a fundamental guiding principle for the study of quasiperiodic models [18–22].

Localization and self-duality also emerge in non-Hermitian quasiperiodic models [23, 24], where the phases and phase transitions are significantly enriched by unique features of non-Hermitian systems such as the spectral topology and non-Hermitian symmetries [25–29]. Like the Hermitian case, the extended-localized duality relation has facilitated the study of various non-Hermitian quasiperiodic models [30–34]. Further, despite the potential boundary sensitivity of eigenstates and eigenspectra in non-Hermitian systems, as in the case of the non-Hermitian skin effect [35–41], it has been considered a universal axiom that localized states in the bulk are insensitive to boundary conditions [1, 32, 33].

In this work, we report the emergence of anomalous, boundary-sensitive localized states and the breakdown of the extended-localized duality relation in non-Hermitian quasiperiodic lattices. Specifically, the boundary-sensitive localized states are Anderson local-

ized in the bulk under the periodic boundary condition (PBC), but become boundary-localized skin modes under the open boundary condition (OBC). Furthermore, the duality relation can be violated, such that the duals of extended states are still extended, provided they are subject to the non-Hermitian skin effect in both models. We show that these counterintuitive properties originate from the interplay of quasiperiodicity and the non-Hermitian skin effect, particularly the non-Hermitian boundary-sensitivity underlying the latter phenomenon. Interestingly, the presence of these anomalous behaviors are closely related to the sign patterns of the Lyapunov exponents [1, 43], which provides insight and control to these phenomena.

Lyapunov exponents and localization.— We start by analyzing the general patterns of Lyapunov exponents for quasiperiodic models. Consider a one-dimensional tight-binding Hamiltonian \hat{H} with total lattice sites N and hopping range M :

$$\hat{H} = \sum_{|n-m| \leq M} J_{n,m} \hat{b}_n^\dagger \hat{b}_m, \quad (1)$$

where \hat{b}_n^\dagger (\hat{b}_n) denote the creation (annihilation) operator on site n , $J_{n,m}$ is the hopping amplitude from site m to n for $n \neq m$, or the on-site potential for $n = m$. The corresponding eigenvalue equations read

$$\sum_{t=-M}^M J_{n,n+t} \psi_{n+t} = E \psi_n, \quad n = 1, 2, \dots, N, \quad (2)$$

where ψ_n is the eigenstate amplitude on site n .

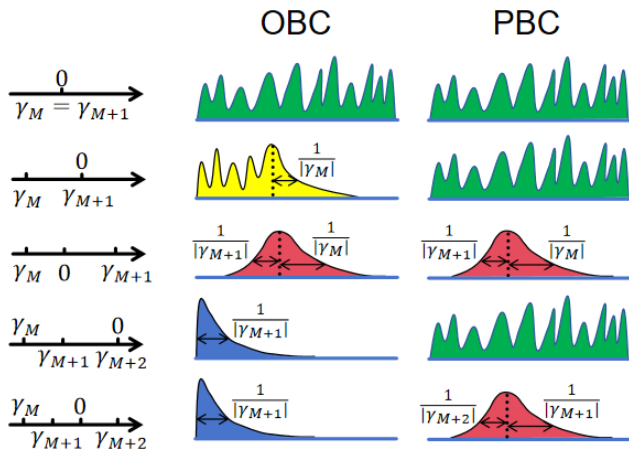


FIG. 1. Schematics of spatial profiles of eigenstates under the OBC and PBC for different sign patterns of the Lyapunov exponents. Green profiles denote non-localized states, red ones denote Anderson localized states, blue denotes boundary-localized skin modes, and yellow denotes states that are extended in one direction and localized in the other [1]. The quantity $1/|\gamma_i|$ indicates the corresponding localization length.

The $2M \times 2M$ transfer matrix with eigenenergy E is

$$T(E) = \prod_{n=1}^N T_n(E), \quad (3)$$

where T_n is defined through $\Psi_n = T_n(E)\Psi_{n-1}$ and $\Psi_n = (\psi_{n+M}, \psi_{n+M-1}, \dots, \psi_{n-M+1})^T$ [44]. Importantly, the eigenvalues of the matrix $\frac{1}{2N} \ln[T^\dagger(E)T(E)]$ in the thermodynamic limit $N \rightarrow +\infty$ correspond to the $2M$ Lyapunov exponents $\gamma_i(E)$ ($i = 1, \dots, 2M$), from which the localization properties of the model can be obtained [45]. For convenience, we sort the Lyapunov exponents in ascending order, with $\gamma_1(E) \leq \dots \leq \gamma_{2M}(E)$. With the prefactor $1/N$ in Eq. (3), the boundary contributions are negligible in the thermodynamic limit. Hence, for a fixed eigenenergy E , one obtains the same set of Lyapunov exponents $\{\gamma_i(E)\}$ under different boundary conditions [1]. Nevertheless, as we show below, localization behaviors of the corresponding eigenstates can be distinct under different boundary conditions.

Let us first consider models without disorder or quasiperiodicity, and the case where the hopping amplitudes in the bulk possess the translational symmetry, with $J_{n,m} = J_{n-m} = t_s$ and $s = n - m$. The corresponding Bloch Hamiltonian is then $H(k) = \sum_{s=-M}^M t_s e^{iks}$. A unified representation of the eigenstates and eigenspectrum, regardless of Hermiticity and boundary conditions, can be formally achieved through the non-Bloch band theory [27, 35, 37], where the factor e^{ik} is replaced by a complex parameter β . For the Hermitian case or for non-Hermitian systems under the PBC, β reduces to the Bloch form of $|\beta| = 1$. But in general, the characteris-

tic equation $\sum_{s=-M}^M t_s \beta^s - E = 0$ admits $2M$ solutions $\beta_i(E)$ (with $i = 1, \dots, 2M$ and labeled in ascending order of $|\beta_i|$). In the thermodynamic limit, eigenspectrum of the system under the OBC is given by eigenenergies E that satisfy $|\beta_M(E)| = |\beta_{M+1}(E)|$. The corresponding eigenstates under the OBC are constructed from the solutions β_M and β_{M+1} , where the Bloch wave factor e^{ikn} is replaced by β_M^n . As a result, localization toward one of the open boundaries, that is, the non-Hermitian skin effect, arises for $|\beta_M| \neq 1$. Crucially, the solutions of the characteristic equation β_i are directly related to the Lyapunov exponents through $\gamma_i(E) = \ln |\beta_i(E)|$ [1]. This means that, under the OBC, the Lyapunov exponents $\gamma_M = \gamma_{M+1}$ are solely responsible for the localization properties of the system. When disorder or quasiperiodicity is introduced, $\gamma_M(E)$ and $\gamma_{M+1}(E)$ are generally no longer equal, but they still dominate the spatial distributions of eigenstates under the OBC [1].

By contrast, under the PBC, the spatial distribution of eigenstates may no longer be dominated by $\gamma_M(E)$ and $\gamma_{M+1}(E)$. In general, different Lyapunov exponents $\gamma_i(E)$ correspond to different decay channels of the eigenstates with eigenenergy E . The channel associated with $\gamma_i(E)$ contribute a factor $e^{\gamma_i(E)n}$ to the spatial profile of the corresponding eigenstate. Hence, in the presence of a vanishing exponent $\gamma_i(E) = 0$, the eigenstate is not Anderson localized, but either extended or critical [33, 43]. Otherwise, in the case that all $\gamma_i(E) \neq 0$, eigenstates at the given E must be localized, since channels with positive γ_i (implying an exponential wave-function growth in n) and those with negative γ_i (n exponential decay in n) must coexist. This is because the $2M$ Lyapunov exponents corresponding to a given eigenenergy E under the PBC cannot all have the same sign, otherwise the monotonic growth (decay) of the wave function would contradict the PBC. Importantly, the localization length on the two sides of the localization center should be governed by the pair of Lyapunov exponents with opposite signs that are closest to zero.

In the conventional case, the Lyapunov exponents are distributed symmetrically with respect to zero. Hence, the dominant decay channels are still governed by γ_M and γ_{M+1} , and the localization behaviors of a given eigenstate are identical under the PBC and OBC. However, by introducing nonreciprocity, the Lyapunov exponents $\gamma_i(E)$ acquire a shift [44], which can break the symmetry in the sign pattern of the Lyapunov exponents. As a result, the Lyapunov exponents governing the spatial distribution of eigenstates can be different under the PBC and OBC. As we show below, this can lead to scenarios beyond the standard non-Hermitian skin effect.

We list the five typical patterns of the Lyapunov exponents in Fig. 1, as well as the corresponding localization scenarios under the OBC and PBC, respectively: (i) $\gamma_M = \gamma_{M+1} = 0$, the eigenstates are extended or critical, regardless of the boundary condition; (ii) $\gamma_M < \gamma_{M+1} =$

0 (or $\gamma_M = 0 < \gamma_{M+1}$), the corresponding eigenstates are extended or critical under the PBC, but is localized in one direction while nonlocal in the other [1]; (iii) $\gamma_M < 0 < \gamma_{M+1}$, the eigenstates are Anderson localized under both OBC and PBC; (iv) $\gamma_M < \gamma_{M+1} < \gamma_{M+2} = 0$ (or $\gamma_{M-1} = 0 < \gamma_M < \gamma_{M+1}$), the eigenstates are extended or critical under the PBC, but boundary-localized under the OBC, as in the standard non-Hermitian skin effect; (v) $\gamma_M < \gamma_{M+1} < 0 < \gamma_{M+2}$ (or $\gamma_{M-1} < 0 < \gamma_M < \gamma_{M+1}$), where the eigenstates are Anderson localized under the PBC, but boundary-localized under the OBC. Here, the most striking case is (v), where the localization is boundary-sensitive. It is distinct from either the conventional Anderson localization, which is unaffected by the boundary, or the conventional non-Hermitian skin effect, where the states are extended or critical under the PBC [33, 46]. Importantly, these boundary-sensitive localized states can be engineered by tuning the pattern of the Lyapunov exponents.

Boundary-sensitive localization.— As an illustrative example, we consider a one-dimensional non-Hermitian quasiperiodic model with both nearest-neighbor and next-nearest-neighbor hoppings ($M = 2$)

$$\hat{H}_1(g, h) = \sum_{1 \leq |m-n| \leq 2} e^{(n-m)g} \hat{b}_m^\dagger \hat{b}_n \frac{\cos[\tau\pi(m+n) + ih]}{|m-n|^3}. \quad (4)$$

Here the irrational number $\tau = (\sqrt{5} - 1)/2$, and the non-Hermitian parameters h and g take real values. The Hamiltonian is a non-Hermitian extension of the self-dual design in Ref. [47], which facilitates our following discussion of its dual model. Notably, by varying g and h , the Lyapunov exponents either acquire a constant shift or becomes wider in range [1, 33, 44], enabling the engineering of particular patterns of the Lyapunov exponents. To characterize localization, we use the fractal dimension (FD) of a normalized eigenstate

$$\text{FD} = \frac{\ln \sum_n |\psi_n|^4}{\ln N}. \quad (5)$$

In the thermodynamic limit, the FD approaches 0 for localized states and 1 for extended states, while it takes intermediate values between 0 and 1 for critical states.

For convenience, we first set $h = 0$. Then, if g also vanishes, \hat{H}_1 becomes Hermitian, and its eigenstates consist of critical and extended states regardless of the boundary condition [47]. This is confirmed in Fig. 2(a1)(b1), where the eigenspectrum remains real with non-vanishing FD. With increasing g , part of the eigenspectrum forms a closed loop on the complex plane under the PBC [see Fig. 2(a2)], in contrast to the OBC case, where the eigenspectrum remains on the real axis [see Fig. 2(b2)]. The latter derives from the similarity transformation $\hat{H}_1(g, 0) = S^{-1} \hat{H}_1(0, 0) S$ in the basis $(\hat{b}_1, \dots, \hat{b}_{2M})^T$ with $S = \text{diag}(e^g, \dots, e^{2Mg})$, which leaves the eigenvalues unchanged for different values of g . Crucially, while

this transformation maps all eigenstates to boundary-localized skin modes under the OBC (under a finite g), it does not apply under the PBC. It follows that, if any bulk localized states are present under the PBC, their localization properties must be different under the OBC.

These boundary-sensitive localized states indeed exist at appropriately chosen g , illustrated in Fig. 2(a2) as the eigenstates on the spectral branch within the loop with real eigenvalues, their FDs approaching unity. In particular, for three randomly chosen eigenstates (marked by colored dots), their spatial distributions show sharp peaks near different localization centers in the bulk [see Fig. 2(c)] under the PBC. Meanwhile, all eigenstates of the system under the OBC are boundary-localized [see Fig. 2(d)].

The emergence of the boundary-sensitive localization can be understood and engineered through the Lyapunov exponents. While their sign pattern encodes the localization behavior of eigenstates with eigenenergy E under different boundary conditions, the Lyapunov exponents at $g = 0$ is related to those at finite g through $\gamma_i(E) \rightarrow \gamma_i(E) - g$ [44], which offers a convenient way to adjust the sign pattern.

For instance, in the Hermitian case [Fig. 2(a1,b1)], the sign pattern is $(-, 0, 0, +)$ (listed as signs from γ_1 to γ_4) for all eigenstates, indicating extended or critical states under either boundary condition. With $g > 0$, the sign pattern is shifted toward negative values. Importantly, for eigenstates on the central branch in Fig. 2(a2), the sign pattern is $(-, -, -, +)$. For these states, the dominant Lyapunov exponents are γ_3 and γ_4 under the PBC, and their opposite signs suggest bulk localization. However, under the OBC, the dominant Lyapunov exponents are γ_2 and γ_3 , which possess the same sign, indicating boundary localization typical of the skin modes. On the other hand, for states on the outer loop in Fig. 2(a2), their corresponding pattern is $(-, -, 0, +)$, consistent with their extended nature. Note that the eigenenergies of these states are dramatically changed under the OBC [see Fig. 2(b2)], wherein their sign pattern becomes $(-, -, -, +)$, indicating boundary localization.

To further confirm the understanding above, we show in Fig. 3 the spatial distribution of eigenstates with a fixed eigenenergy but under different g . In all cases, sharp peaks are observed near the localization centers, with the localization lengths on the two sides matching $\gamma_3(E)$ and $\gamma_4(E)$, respectively.

As such, these boundary-sensitive localized states necessarily exist for nonvanishing sets of Lyapunov exponents with an asymmetric sign pattern, that is, with an unequal number of positive and negative exponents. For this to occur, three key ingredients are required: (i) quasiperiodicity, which enables the emergence of localization; (ii) non-Hermitian skin effect, which breaks the symmetry of the sign pattern; and (iii) long-range hopping, which generates multiple Lyapunov exponents

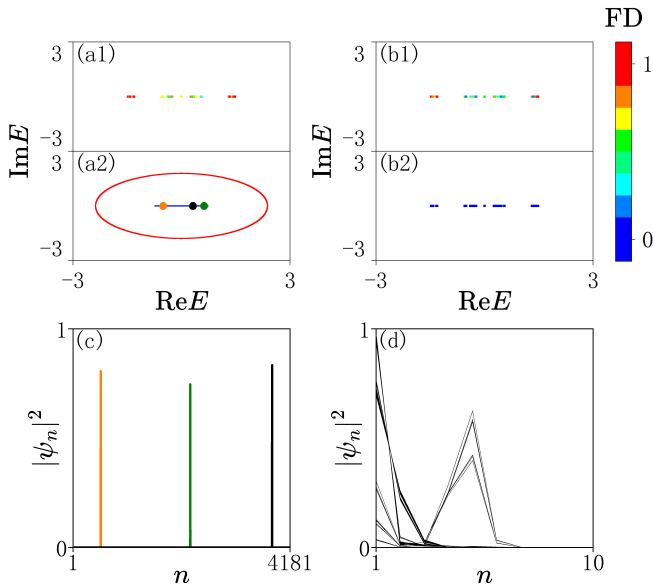


FIG. 2. (a)(b) Eigenspectra of $\hat{H}_1(g, 0)$ under (a) PBC and (b) OBC, respectively, where the color indicates the FD of the corresponding eigenstate. The parameters are (a1)(b1) $g = 0$ and (a2)(b2) $g = 1$. (c) Spatial distributions of typical localized states, marked in (a2) with matching colors. (d) Spatial distributions of every tenth eigenstate in (b2). These eigenstates are all localized toward the boundary $n = 1$. The system size for all calculations is $N = 4181$.

(≥ 4). Physically, the boundary-sensitive localization under the PBC is akin to the inner skin effect in Ref. [48], where the incompatibility of the PBC and quasiperiodicity effectively generates inner boundaries in the bulk, which becomes the various localization centers due to the non-Hermitian boundary sensitivity. Whereas under the OBC, nonreciprocal hoppings make eigenstates localize at the real physical boundaries. These considerations suggest that boundary-sensitive localization should be a common phenomenon in non-Hermitian quasiperiodic systems with long-range hopping.

Breakdown of the duality relation.— The interplay of non-Hermiticity and quasiperiodicity also has interesting implications for the nonlocal state under the PBC. To see this, we examine the dual model of $H_1(g, h)$ [44]

$$\hat{H}_2(g, h) = \sum_m (e^{-h} \hat{b}_m^\dagger \hat{b}_{m+1} + e^h \hat{b}_{m+1}^\dagger \hat{b}_m) \sum_{s=1}^2 \frac{\cos[\tau s \pi (2m+1) + i s g]}{s^3}, \quad (6)$$

which features only nearest-neighbor hopping ($M = 1$) but two quasiperiodic modulations parameterized by s . From a numerical perspective, while the duality strictly holds in the thermodynamic limit for irrational τ , it exactly holds in finite systems by imposing PBC with system size $N = F_j$ and adopting the rational approximation $\tau_{\text{RA}} = F_{j-1}/F_j$, where F_j is the j th Fibonacci num-

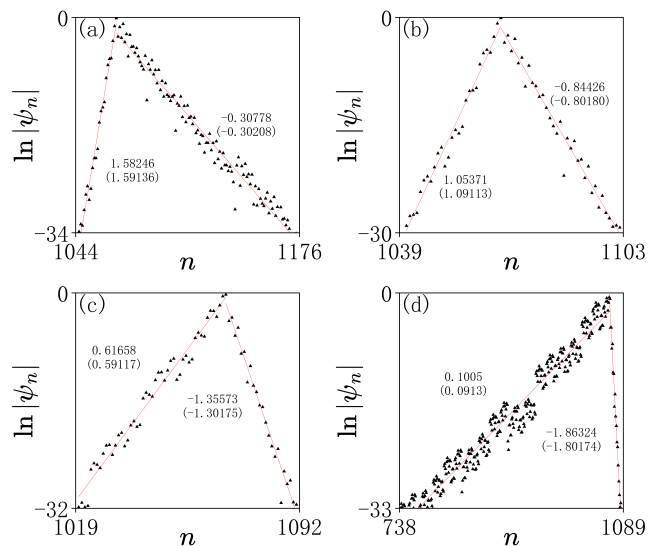


FIG. 3. Spatial distributions for eigenstates of $\hat{H}_1(g, 0)$, with $E = 0.025$, and (a) $g = 0.5$, (b) $g = 1$, (c) $g = 1.5$, (d) $g = 2$. Black dots represent numerical results, and red lines denote linear fits. The numbers outside the brackets represent the localization strengths obtained from the linear fits, and those within the brackets represent the corresponding $\gamma_3(E)$ and $\gamma_4(E)$. For all calculations, the system size is $N = 10946$ and the PBC is imposed.

ber [44]. By design, both H_1 and H_2 possess the non-Hermitian skin effect under finite g and h .

According to the conventional extended-localized duality relation, an extended (localized) state in $H_1(g, h)$ should be mapped to a localized (extended) state in $H_2(g, h)$, whereas critical states remain critically localized in both models. However, this duality relation does not always hold. In Fig. 4(a)(b), we show the PBC eigenspectra of both models, respectively, with a fixed g and varying h . When h is small, the eigenvalues in the complex plane form two concentric rings. Under \hat{H}_1 , the inner (outer) ring corresponds to localized (extended) states, while for \hat{H}_2 the situation is reversed. In this regime, the duality relation holds well. As h increases, the two rings start to merge, and the duality relation breaks down in the overlapping region, although it still holds in the remaining parts of the spectrum. In Fig. 4(a3)(b3), the rings completely overlap, and all eigenstates of both models are extended (with their FD approaching 1), violating the aforementioned duality relation.

To confirm the observations above, we show typical spatial profiles of eigenstates of \hat{H}_1 in Fig. 4(c), and those of \hat{H}_2 but with the same eigenenergies in Fig. 4(d). We also compute the corresponding sign patterns of the Lyapunov exponents. In Fig. 4(c1)(c2) and (d1)(d2), the duality relation still holds, and the sign patterns are $(-, -, -, +)$ and $(0, +)$, consistent with the extended-localized duality relation. By contrast, the sign patterns

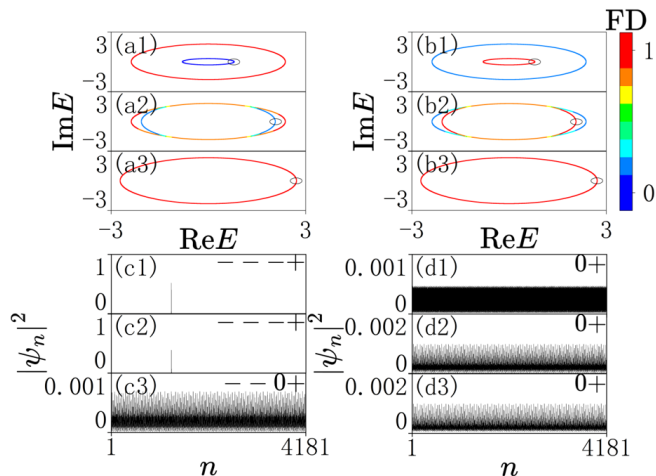


FIG. 4. (a)(b) Eigenspectra of (a) $\hat{H}_1(1, h)$ and (b) $\hat{H}_2(1, h)$, respectively, under the PBC, with color contours indicating the FD of the corresponding eigenstates. The parameters are (a1)(b1) $h = 0.1$, (a2)(b2) $h = 0.4$, and (a3)(b3) $h = 0.6$. (c1–c3)(d1–d3) Spatial distributions of the eigenstates marked by circles on the real axis in (a1–a3) and (b1–b3), respectively. The corresponding sign patterns of $\gamma_i(E)$ are indicated in the upper-right corners of (c)(d). For all calculations, the system size is fixed at $N = 4181$ under the PBC, with the irrational number τ is approximated by $\tau_{\text{RA}} = 2584/4181$.

become $(-, -, 0, +)$ and $(0, +)$ in Fig. 4(c3)(d3), as both eigenstates are extended. This conclusion is supported by finite-size-scaling analysis [44], which confirms the breakdown of the duality relation in the thermodynamic limit.

The breakdown of duality is counterintuitive, but not unreasonable. Since the dual transformation is essentially a Fourier transformation, the mapping from localized states to extended states can be understood as a manifestation of the Heisenberg–Pauli–Weyl uncertainty principle [49]. However, the Fourier transform of an extended state can remain extended without violating this principle. Note that the observed breakdown of duality always occurs when both \hat{H}_1 and \hat{H}_2 possess nonlocal eigenstates at the same energy E . From the perspective of Lyapunov exponents, this means the presence of vanishing exponents in both Hamiltonians. Again, this is facilitated by the non-Hermitian skin effect, which breaks the symmetry in the sign pattern of the Lyapunov exponents.

Discussion.— We have uncovered anomalous boundary-sensitive localization and the breakdown of the extended-localized duality relation in non-Hermitian quasiperiodic lattices. While both phenomena are facilitated by the interplay of non-Hermitian skin effect and quasiperiodicity, we illustrate how each can be engineered and analyzed through the sign patterns of the Lyapunov exponents. From the perspective of Lyapunov exponents, we argue that these phenomena are generic in non-Hermitian quasiperiodic systems

with long-range hopping. While our models can be implemented on existing quantum simulation platforms such as the Rydberg atoms [47], our work highlights the dramatic impact of non-Hermiticity on quasiperiodic systems.

This work is supported by the National Natural Science Foundation of China (Grant No. 12374479), and the Innovation Program for Quantum Science and Technology (Grant No. 2021ZD0301904). T.L. is supported by National Natural Science Foundation of China (Grant No.12504189), and the Guangdong Basic and Applied Basic Research Foundation (Grant No.2026A1515012098).

* tianyu@scnu.edu.cn

† wyz@ustc.edu.cn

- [1] P. W. Anderson, Phys. Rev. **109**, 1492 (1958).
- [2] E. Abrahams, P. W. Anderson, D. C. Licciardello, and T. V. Ramakrishnan, Phys. Rev. Lett. **42**, 673 (1979).
- [3] P. A. Lee and T. V. Ramakrishnan, Rev. Mod. Phys. **57**, 287 (1985).
- [4] A. Lagendijk, B. Tiggelen, and D. S. Wiersma, Phys. Today **62**, 24 (2009).
- [5] B. Kramer and A. MacKinnon, Rep. Prog. Phys. **56**, 1469 (1993).
- [6] P. G. Harper, Proc. Phys. Soc. London Sect. A **68**, 874 (1955).
- [7] M. Kohmoto, Phys. Rev. Lett. **51**, 1198 (1983).
- [8] G. Roati, C. D’Errico, L. Fallani, M. Fattori, C. Fort, M. Zaccanti, G. Modugno, and M. Inguscio, Nature (London) **453**, 895 (2008).
- [9] D. J. Thouless, Phys. Rev. Lett. **61** 2141 (1988).
- [10] X. Deng, S. Ray, S. Sinha, G. V. Shlyapnikov, and L. Santos, Phys. Rev. Lett. **123**, 025301 (2019).
- [11] J. Wang, X.-J. Liu, X. Gao, and H. Hu, Phys. Rev. B **93**, 104504 (2016).
- [12] A. Szabó and U. Schneider, Phys. Rev. B **101**, 014205 (2020).
- [13] S. Aubry and G. André, Ann. Isr. Phys. Soc. **3**, 133 (1980).
- [14] S. Y. Jitomirskaya, Ann. Math. **150**, 1159 (1999).
- [15] M. Modugno, New J. Phys. **11**, 033023 (2009).
- [16] J. Biddle and S. Das Sarma, Phys. Rev. Lett. **104**, 070601 (2010).
- [17] S. Ganeshan, J. H. Pixley, and S. Das Sarma, Phys. Rev. Lett. **114**, 146601 (2015).
- [18] S. Gopalakrishnan, Phys. Rev. B **96**, 054202 (2017).
- [19] D. K. Sahu, A. P. Acharya, D. Choudhuri, and S. Datta, Phys. Rev. B **104**, 054202 (2021).
- [20] M. Gonçalves, B. Amorim, E. V. Castro, and P. Ribeiro, Phys. Rev. Lett. **131**, 186303 (2023).
- [21] H.-T. Hu, X. Lin, A.-M. Guo, G. Guo, Z. Lin, and M. Gong, Phys. Rev. Lett. **134**, 246301 (2025).
- [22] S.-Z. Li, Y.-C. Zhang, Y. Wang, S. Zhang, S.-L. Zhu, and Z. Li, Sci. China-Phys. Mech. Astron. **69**, 217212 (2026).
- [23] S. Longhi, Phys. Rev. Lett. **122**, 237601 (2019).
- [24] H. Jiang, L.-J. Lang, C. Yang, S.-L. Zhu, and S. Chen, Phys. Rev. B **100**, 054301 (2019).
- [25] Z. Gong, Y. Ashida, K. Kawabata, K. Takasan, S. Hi-

- gashikawa, and M. Ueda, *Phys. Rev. X* **8**, 031079 (2018).
- [26] K. Kawabata, K. Shiozaki, M. Ueda, and M. Sato, *Phys. Rev. X* **9**, 041015 (2019).
- [27] K. Kawabata, N. Okuma, and M. Sato, *Phys. Rev. B* **101**, 195147 (2020).
- [28] N. Okuma, K. Kawabata, K. Shiozaki, and M. Sato, *Phys. Rev. Lett.* **124**, 086801 (2020).
- [29] E. J. Bergholtz, J. C. Budich, and F. K. Kunst, *Rev. Mod. Phys.* **93**, 015005 (2021).
- [30] Q.-B. Zeng, Y.-B. Yang, and Y. Xu, *Phys. Rev. B* **101**, 020201(R) (2020).
- [31] Y. Liu, X.-P. Jiang, J. Cao, and S. Chen, *Phys. Rev. B* **101**, 174205 (2020).
- [32] Y. Liu, Y. Wang, Z. Zheng, and S. Chen, *Phys. Rev. B* **103**, 134208 (2021).
- [33] Y. Liu, Q. Zhou, and S. Chen, *Phys. Rev. B* **104**, 024201(2021).
- [34] S. Longhi, *Phys. Rev. B* **100**, 125157 (2019).
- [35] S. Yao and Z. Wang, *Phys. Rev. Lett.* **121**, 086803 (2018).
- [36] F. Song, S. Yao, and Z. Wang, *Phys. Rev. Lett.* **123**, 170401 (2019).
- [37] K. Yokomizo and S. Murakami, *Phys. Rev. Lett.* **123**, 066404 (2019).
- [38] K. Zhang, Z. Yang, and C. Fang, *Phys. Rev. Lett.* **125**, 126402 (2020).
- [39] Y. Ashda, Z. Gong, and M. Ueda, *Adv. Phys.* **69**, 249 (2020).
- [40] X. Zhang, T. Zhang, M.-H. Lu, and Y.-F. Chen, *Advances in Physics: X* **7**, 2109431 (2022).
- [41] N. Okuma and M. Sato, *Annu. Rev. Condens. Matter Phys.* **14**, 83 (2023).
- [42] K. Sun and H. Hu, arXiv:2507.09447 (2025).
- [43] A. Avila, *Acta Math.* **215**, 1 (2015).
- [44] See Supplemental Material for details.
- [45] K. H. Hoffmann and M. Schreiber (eds.), *Computational Physics* (Springer, Berlin, Heidelberg, 1996).
- [46] X. Cai, *Phys. Rev. B* **106**, 214207 (2022).
- [47] W. Wang, W. Yi, and T. Li, *Phys. Rev. B* **112**, L140201 (2025).
- [48] S. Manna and B. Roy, *Commun Phys* **6**, 10 (2023).
- [49] P. Ciatti, F. Ricci, and M. Sundari, *Advances in Mathematics*, **215** (2007).

Supplemental Material for “Boundary-sensitive localization and ineffective duality in one-dimensional non-Hermitian quasicrystals”

In this Supplemental Material, we provide more details on (I) Derivation of the transfer matrix; (II) Nonreciprocity-induced shift of Lyapunov exponents; (III) Duality between \hat{H}_1 and \hat{H}_2 ; (IV) Scaling analysis of the boundary-sensitive localized states and dual extended states.

DERIVATION OF THE TRANSFER MATRIX

Starting from the eigenvalue equations of \hat{H} in the main text

$$\sum_{t=-M}^M J_{n,n+t} \psi_{n+t} = E \psi_n, \quad n = 1, 2, \dots, N, \quad (\text{S1})$$

one can rewrite these eigenvalue equations in terms of a $2M \times 2M$ transfer matrices

$$\begin{pmatrix} \psi_{n+M} \\ \psi_{n+M-1} \\ \vdots \\ \psi_{n-M+1} \end{pmatrix} = T_n \begin{pmatrix} \psi_{n+M-1} \\ \psi_{n+M-2} \\ \vdots \\ \psi_{n-M} \end{pmatrix}, \quad (\text{S2})$$

with

$$T_n(E) = \begin{pmatrix} -\frac{J_{n,n+M-1}}{J_{n,n+M}} & -\frac{J_{n,n+M-1}}{J_{n,n+M}} & \dots & -\frac{J_{n,n+1}}{J_{n,n+M}} & \frac{E-J_{n,n}}{J_{n,n+M}} & -\frac{J_{n,n-1}}{J_{n,n+M}} & \dots & -\frac{J_{n,n-M}}{J_{n,n+M}} \\ 1 & & & & & & & \\ & 1 & & & & & & \\ & & \ddots & & & & & \\ & & & 1 & & & & \\ & & & & 1 & & & \\ & & & & & 1 & & \\ & & & & & & \ddots & \end{pmatrix}, \quad n = 1, 2, \dots, N. \quad (\text{S3})$$

Note that this matrix has nonzero elements only on the first row and the subdiagonal, and propagates the wave function by one lattice site at each step.

By introducing the supercell formalism and rearranging the eigenvalue equations in Eq. (S1), one can obtain alternatively [1],

$$\begin{pmatrix} \tilde{\Psi}_{n+1} \\ \tilde{\Psi}_n \end{pmatrix} = \tilde{T}_n \begin{pmatrix} \tilde{\Psi}_n \\ \tilde{\Psi}_{n-1} \end{pmatrix}, \quad (\text{S4})$$

where $\tilde{\Psi}_n = (\psi_{nM}, \psi_{nM-1}, \dots, \psi_{(n-1)M+1})^T$ denotes the supercell wave function.

The supercell transfer matrix \tilde{T}_n propagates the wave function by one supercell at each step, in contrast to $T_n(E)$. The two transfer matrices are related through

$$\tilde{T}_n = \prod_{m=1}^M T_{(n-1)M+m}. \quad (\text{S5})$$

It should be noted that these two transfer matrices yield the same Lyapunov exponents.

NONRECIPROCITY-INDUCED SHIFT OF LYAPUNOV EXPONENTS

When the parameter g in $\hat{H}_1(g, h)$ of the main text is switched on from 0 to a nonzero value, the hopping coefficients $J_{n,m}(g)$ in Eq. (S1) are modified as

$$J_{n,m}(g) = e^{(m-n)g} J_{n,m}(g=0). \quad (\text{S6})$$

This induces the following transformation of the single-site transfer matrix:

$$T_n(g, E) = e^{-g} S T_n(g = 0, E) S^{-1}, \quad (\text{S7})$$

where $S = \text{diag}(e^g, e^{2g}, \dots, e^{2Mg})$.

Accordingly, the full transfer matrix becomes

$$T(g, E) = \prod_{n=1}^N T_n(g, E) = e^{-Ng} S \prod_{n=1}^N T_n(g = 0, E) S^{-1} = e^{-Ng} S T(g = 0, E) S^{-1}. \quad (\text{S8})$$

It then follows that

$$\frac{1}{2N} \ln[T^\dagger(g, E)T(g, E)] = \frac{1}{2N} \ln[ST^\dagger(g = 0, E)T(g = 0, E)S^{-1}] - g. \quad (\text{S9})$$

Since the Lyapunov exponents $\gamma_i(E)$ are given by the eigenvalues of $\frac{1}{2N} \ln[T^\dagger(E)T(E)]$ in the limit $N \rightarrow +\infty$, and similarity transformations do not change eigenvalues, the Lyapunov exponents are shifted according to

$$\gamma_i(g, E) = \gamma_i(g = 0, E) - g, \quad i = 1, 2, \dots, 2M. \quad (\text{S10})$$

DUALITY BETWEEN \hat{H}_1 AND \hat{H}_2

In this section, we demonstrate the duality between \hat{H}_1 and \hat{H}_2 in the main text. For completeness, we rewrite them here:

$$\hat{H}_1(g, h) = \sum_{1 \leq |m-n| \leq 2} e^{(n-m)g} \hat{b}_m^\dagger \hat{b}_n \frac{\cos[\tau\pi(m+n) + ih]}{|m-n|^a}, \quad (\text{S11})$$

and

$$\hat{H}_2(g, h) = \sum_m (e^{-h} \hat{b}_m^\dagger \hat{b}_{m+1} + e^h \hat{b}_{m+1}^\dagger \hat{b}_m) \sum_{s=1}^2 \frac{\cos[\tau s \pi(2m+1) + isg]}{s^a}. \quad (\text{S12})$$

Applying the dual transformation

$$\hat{b}_n = \frac{1}{\sqrt{N}} \sum_{k=1}^N e^{-2i\pi\tau nk} \hat{b}_k, \quad n = 1, 2, \dots, N, \quad (\text{S13})$$

we obtain

$$\begin{aligned}
\hat{H}_1(g, h) &= \sum_{1 \leq |m-n| \leq 2} e^{(n-m)g} \hat{b}_m^\dagger \hat{b}_n \frac{\cos[\tau\pi(m+n) + ih]}{|m-n|^a} \\
&= \sum_{t=\pm 1, \pm 2} \sum_n e^{-tg} \hat{b}_{n+t}^\dagger \hat{b}_n \frac{\cos[\tau\pi(2n+t) + ih]}{|t|^a} \\
&= \frac{1}{2N} \sum_{t=\pm 1, \pm 2} \frac{e^{-tg}}{|t|^a} \sum_{nkl} \hat{b}_k^\dagger \hat{b}_l e^{2i\pi\tau(n+t)k} e^{-2i\pi\tau nl} (e^{i\tau\pi(2n+t)} e^{-h} + e^{-i\tau\pi(2n+t)} e^h) \\
&= \frac{1}{2N} \sum_{t=\pm 1, \pm 2} \frac{e^{-tg}}{|t|^a} \sum_{nkl} \hat{b}_k^\dagger \hat{b}_l (e^{-h} e^{2\pi i\tau n(k-l+1)} e^{\pi i\tau t(2k+1)} + e^h e^{2\pi i\tau n(k-l-1)} e^{\pi i\tau t(2k-1)}) \\
&= \frac{1}{2} \sum_{t=\pm 1, \pm 2} \frac{e^{-tg}}{|t|^a} \sum_{kl} \left(e^{-h} e^{\pi i\tau t(2k+1)} \frac{1}{N} \sum_n \hat{b}_k^\dagger \hat{b}_l e^{2\pi i\tau n(k-l+1)} \right. \\
&\quad \left. + e^h e^{\pi i\tau t(2k-1)} \frac{1}{N} \sum_n \hat{b}_k^\dagger \hat{b}_l e^{2\pi i\tau n(k-l-1)} \right) \\
&= \frac{1}{2} \sum_{t=\pm 1, \pm 2} \frac{e^{-tg}}{|t|^a} \sum_{kl} (e^{-h} e^{\pi i\tau t(2k+1)} \hat{b}_k^\dagger \hat{b}_l \delta_{k,l-1} + e^h e^{\pi i\tau t(2k-1)} \hat{b}_k^\dagger \hat{b}_l \delta_{k,l+1}) \\
&= \frac{1}{2} \sum_{t=\pm 1, \pm 2} \frac{e^{-tg}}{|t|^a} \sum_l (e^{-h} e^{\pi i\tau t(2l+1)} \hat{b}_l^\dagger \hat{b}_{l+1} + e^h e^{\pi i\tau t(2l+1)} \hat{b}_{l+1}^\dagger \hat{b}_l) \\
&= \sum_l (e^{-h} \hat{b}_l^\dagger \hat{b}_{l+1} + e^h \hat{b}_{l+1}^\dagger \hat{b}_l) \sum_{t=\pm 1, \pm 2} \frac{e^{-tg} e^{\pi i\tau t(2l+1)}}{2|t|^a} \\
&= \sum_l (e^{-h} \hat{b}_l^\dagger \hat{b}_{l+1} + e^h \hat{b}_{l+1}^\dagger \hat{b}_l) \sum_{t=1}^2 \frac{\cos[\tau t\pi(2l+1) + itg]}{t^a}, \tag{S14}
\end{aligned}$$

which reproduces exactly $\hat{H}_2(g, h)$ in the dual basis, thus confirming the duality between $H_1(g, h)$ and $H_2(g, h)$. Here, $\delta_{k,l}$ is the Kronecker delta. In the derivation, we have used the identity

$$\lim_{N \rightarrow +\infty} \frac{1}{N} \sum_{n=1}^N e^{2\pi i\tau n(k-l)} = \delta_{k,l}, \tag{S15}$$

which holds strictly for irrational τ .

While the above derivation strictly holds in the thermodynamic limit and for irrational τ , the duality relation can also be realized for finite systems under appropriate conditions.

By imposing periodic boundary conditions $\hat{b}_{n+N} = \hat{b}_n$ for a finite system size $N = F_j$ and adopting the rational approximation $\tau_{\text{RA}} = F_{j-1}/F_j$, where F_j is the j -th Fibonacci number defined recursively as $F_j = F_{j-1} + F_{j-2}$ with $F_1 = 0$ and $F_2 = 1$, the derivation above remains valid.

Specifically, under the dual transformation

$$\hat{b}_n = \frac{1}{\sqrt{N}} \sum_{k=1}^N e^{-2i\pi\tau_{\text{RA}}nk} \hat{b}_k, \quad n = 1, 2, \dots, N, \tag{S16}$$

and using the identity

$$\frac{1}{N} \sum_{n=1}^N e^{2\pi i\tau_{\text{RA}}n(k-l)} = \delta_{k,l}, \tag{S17}$$

the derivation in Eq. (S14) still holds. Such a construction of duality in finite-size systems facilitate numerical calculations.

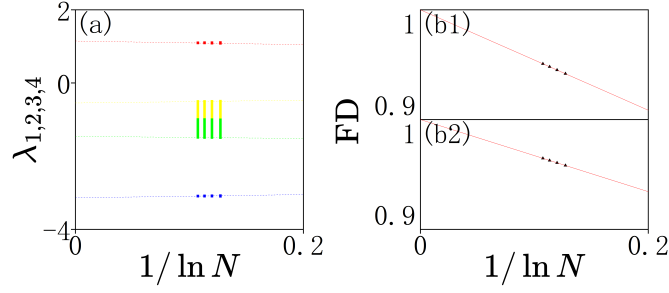


Fig S1. (a) Lyapunov exponents of the boundary-sensitive localized states in Fig. 2(a3) of the main text, plotted as functions of the inverse logarithm of the system size, $1/\ln N$. Points of different colors correspond to γ_1 (red), γ_2 (yellow), γ_3 (green), and γ_4 (blue), respectively. Dashed lines show linear fittings for the smallest γ_1 , the largest γ_2 , the smallest γ_3 , and the largest γ_4 for each N . The sign pattern $(---+)$ of the Lyapunov exponents remains unchanged with increasing system size. (b) Scaling analysis of the FD for a dual pair of eigenstates of the models H_1 and H_2 , marked by circles on the real axis in Fig. 4(a3) and (b3) of the main text. Black dots are numerical results, and red lines are linear fittings. Both FDs approach 1 as N approaches infinity, confirming that these states are extended.

SCALING ANALYSIS OF THE BOUNDARY-SENSITIVE LOCALIZED STATES AND DUAL EXTENDED STATES

In this section, we perform a scaling analysis of the boundary-sensitive localized states in Fig. 2(a3) and the dual extended states in Fig. 4(a3) and (b3) of the main text. As shown in Fig. S1(a), the sign pattern $(---+)$ of the Lyapunov exponents for the boundary-sensitive localized states remains unchanged with increasing system size, indicating that these localized states are not artifacts from finite-size effects. Figure S1(b) shows the scaling of the fractal dimensions (FDs) of two dual extended eigenstates of H_1 and H_2 . Both FDs approach 1 as N increases, confirming that these states are indeed extended in the thermodynamic limit.

* tianyuli@m.scnu.edu.cn

† wyz@ustc.edu.cn

[1] K. Sun and H. Hu, arXiv:2507.09447 (2025).